IEEE Access
Multidisciplinary | Rapid Review | Open Access Journal

Received 26 May 2024, accepted 13 July 2024, date of publication 17 July 2024, date of current version 25 July 2024.

Digital Object Identifier 10.1109/ACCESS.2024.3430096

RESEARCH ARTICLE

Implicit Uniform Rational Spline Reconstruction Method With Regularization Term

SHENGHAN HUANG
Department of Mathematics, South China University of Technology, Guangzhou 510640, China
e-mail: 202130135014@mail.scut.edu.cn

This work was supported by the National College Student Innovation and Entrepreneurship Training Program under Grant 202310561144.

ABSTRACT To improve the accuracy of implicit curve reconstruction and reduce the occurrence of supplementary zero-level sets during the reconstruction process, we propose an implicit curve fitting method with a regularization term based on uniform rational B-splines. First, an implicit uniform rational spline reconstruction model is established using an implicit B-spline reconstruction method. Second, by introducing internal and external offset points during reconstruction, the occurrence of supplementary zero-level sets is reduced, and a regularization term is added to adjust the structure of the reconstructed surface during iteration. Finally, a comparison is made with the I-PIA(implicit progressive iterative approximation) method under the same iteration steps and the same iteration accuracy. The proposed method demonstrates enhanced reconstruction precision and effectively ameliorates the characteristics of the reconstructed surface, which shows robustness in noisy datasets.

INDEX TERMS Implicit curve reconstruction, regularization term, uniform rational splines.

I. INTRODUCTION

Curve reconstruction is a widely studied topic in computer-aided geometric design. Parameterization and implicit representation emerge as two prevalent methodologies for depicting curves, particularly when confronted with scattered and disordered data points. Determining the parameterization of data points is a formidable task when handling scattered data, whereas implicit representation obviates the necessity for parameterization.

Implicit reconstruction methods include implicit T-splines [1], RBF(radial basis function) [2], implicit B-splines [3], etc. Among these methods, the B-spline reconstruction approach requires fewer parameters and is faster for curve or surface reconstruction. However, it may not adapt well to complex shapes. In contrast, rational splines provide a more flexible way to describe point cloud data with complex geometric features. The study of NURBS curves and surfaces [4] has also attracted the attention of many researchers. In [5] and [6], Costa et al. formulated and solved the curve and surface fitting problem using a basis spline and non-uniform rational basis spline entities in the most general case. In particular, the problem is solved by considering, as design variables, not only the continuous parameters of the entity but also the integer ones. With the advancement of intelligent algorithms, more algorithms [7], [8] have been applied to rational spline-based curves and surface reconstruction.

The progressive iterative approximation (PIA) method is a widely used approach for curve and surface fitting, which interpolates data points by generating a series of constraints on control points, and has been successfully applied in various fields. In 1975, Qi et al. [9] discovered the PIA property of uniform cubic B-splines, and de Boor [10] later proved the convergence of the PIA. In 2004, Lin et al. [11] proved the profit and loss correction properties of non-uniform cubic B-spline curves and surfaces, and in 2005 [12], Lin et al. proved that curves and surfaces represented by normalized weight basis functions, such as B-splines and NURBS, also possess PIA properties. Traditional PIA methods converge slowly when dealing with large-scale datasets. To address this issue, Lin and Zhang proposed the E-PIA method [13] and Deng and Lin proposed the LSPIA method [14]. These methods effectively reduce

The associate editor coordinating the review of this manuscript and approving it for publication was Fabian Khateb.

computational costs when processing large-scale data and have been proven to converge.

In implicit reconstruction methods, supplementary zero-level sets often appear because the value of the implicit function depends only on the sampled points and their vicinity [15] and lacks constraints in other regions. The occurrence of supplementary zero-level sets is a challenging problem for implicit curves and surface reconstructions. To reduce the occurrence of supplementary zero sets during fitting, Rouhani and Sappa [16] introduced tensor terms to reduce the extra zero sets. To address this issue, Liu et al. [17] proposed a total variation regularization model in 2017. In 2020, Hamza et al. [18] proposed the I-PIA method, which effectively eliminated pseudo-patches. Based on the I-PIA method, Wang [19] proposed the IR-PIA method in 2022, which has faster convergence speed and lower computational complexity than the I-PIA method. Additionally, [20] proposed an Euler elastica regularization term that significantly enhances reconstruction. Furthermore, [21] added a normal term to control the normal error of the curve. These regularization terms are crucial for enhancing the efficiency and feature refinement of the curves or surface reconstructions.

This paper proposes a method that replaces B-spline basis functions with uniform rational spline basis functions and incorporates internal and external offset points. Furthermore, a regularization term is introduced to control the overall oscillation of the reconstructed surface and prevent the occurrence of supplementary zero-level sets during the iteration process. The PIA property of rational splines is utilized to iteratively reconstruct the surface until the iteration requirements are met. The results show that using uniform rational spline basis functions instead of B-spline basis functions can achieve higher accuracy than the I-PIA method with the same number of iterations. Additionally, when comparing the algorithm with and without the regular term under the same iteration error, it is demonstrated that this method effectively reduces the oscillation phenomenon of the reconstructed surface and minimizes the occurrence of supplementary zero-level sets.

The remainder of this paper is organized as follows. Section II introduces the implicit B-spline curve reconstruction method, and Section III introduces the method of implicit uniform rational B-spline curve reconstruction. In Section IV, we introduce the supplementary zero-level set and propose a regularization term to reduce the oscillation of the reconstructed surface. A series of numerical experiments are used to demonstrate the effectiveness of the proposed method in Section V. Sensitivity analysis is employed to illustrate the stability of the optimization problem, while the algorithm shows robustness in data sets with noise. Finally, Section VI concludes the paper.

II. IMPLICIT CURVE RECONSTRUCTION WITH B-SPLINE

A. RECONSTRUCTION MODEL

This section introduces the implicit B-spline curve reconstruction model. Given a set of unordered two-dimensional point cloud data:

$$\{P_i = (x_i, y_i), i = 1, 2, \ldots, m\}, \tag{1}$$

and their corresponding unit normal vectors: $\{\mathbf{n}_i, i = 1, 2, \ldots, m\}$. To fulfill (1), we need to find a nonzero implicit function $f(x, y)$ such that $f(P_i) = 0$. $f(x, y)$ is a function defined on $\Omega \subseteq \mathbb{R}^2$:

$$f(x, y) = \sum_{i=1}^{N} \sum_{j=1}^{M} C_{ij} B_i(x) B_j(y), \tag{2}$$

where C_{ij} are the control coefficients and $B_i(x)$, $B_j(y)$ are the cubic B-spline basis functions defined on the uniform nodes. Thus, the resulting implicit curve can be expressed as

$$z_f = \{(x, y) \in \Omega \subseteq \mathbb{R}^2 : f(x, y) = 0\}. \tag{3}$$

Because the number of unknowns in the equations formed by all points satisfying (3) is usually greater than the number of data points, supplementary zero-level sets are present in the reconstructed result. To reduce the presence of supplementary zero-level sets in the final fitted surface, we propose adding internal and external offset points to the dataset as follows:

$$\begin{cases} P_l = P_i + d_1 \mathbf{n}_i, & l = m + i, \quad i = 1, 2, \ldots, m, \\ P_k = P_i - d_2 \mathbf{n}_i, & k = 2m + i, \quad i = 1, 2, \ldots, m, \end{cases} \tag{4}$$

where d_1 and d_2 are internal and external distances, respectively. Let ϵ_1,ϵ_2 be the value of the implicit function at internal and external offset points,i.e.,

$$\begin{cases} f(P_l) = \epsilon_1 \\ f(P_k) = \epsilon_2. \end{cases} \tag{5}$$

The problem of implicit curve reconstruction with B-spline is to find a nonzero function $f(x, y)$ to minimize the square error function:

$$\begin{aligned} E(C) = &\sum_{i=1}^{m} \|f(P_i)\|_2^2 \\ &+ \sum_{l=m+1}^{2m} \|f(P_l) - \epsilon_1\|_2^2 \\ &+ \sum_{k=2m+1}^{3m} \|f(P_k) - \epsilon_2\|_2^2. \end{aligned} \tag{6}$$

We fixed the uniform node vector, and our method to modify the shape of the curve involved moving the control coefficients. By considering the control coefficients C_{ij} as optimization variables, our problem is essentially equivalent to the following optimization problem:

$$\arg\min_{C} E(C). \tag{7}$$

B. ITERATIVE PROCESS

Define the initial implicit function as follows:

$$f^{(0)}(x,y)=\sum_{i=1}^{N}\sum_{j=1}^{M}C_{ij}^{(0)}B_i(x)B_j(y), \tag{8}$$

where N and M correspond to the number of basis functions in the x and y directions, respectively. N and M are typically chosen based on experience or the distribution of data points; their selection and impact are discussed in [22] and [23].

Let $C=[C_{11},C_{12},\ldots,C_{NM}]^{\mathrm{T}}$, and collocation matrix of the basis functions be

$$B_1=\begin{bmatrix} B_1(x_1)B_1(y_1),\cdots & B_1(x_1)B_M(y_1),\cdots & B_N(x_1)B_M(y_1)\\ B_1(x_2)B_1(y_2),\cdots & B_1(x_2)B_M(y_2),\cdots & B_N(x_2)B_M(y_2)\\ \vdots & \vdots & \vdots\\ B_1(x_m)B_1(y_m),\cdots & B_1(x_m)B_M(y_m),\cdots & B_N(x_m)B_M(y_m)\end{bmatrix},$$

thus

$$\begin{bmatrix} f^{(0)}(x_1,y_1)\\ f^{(0)}(x_2,y_2)\\ \cdots\\ f^{(0)}(x_m,y_m)\end{bmatrix}=B_1C^{(0)}.$$

Let $\delta_i^{(0)}$ be the difference vectors for the data points, i.e.,

$$\delta_i^{(0)}=0-f(x_i,y_i),\quad i=1,2,\ldots,m.$$

Additionally, let $\Delta_{ij}^{(0)}, i=1,2,\ldots,N, j=1,2,\ldots,M$ be the difference vectors for the control coefficients,i.e.,

$$\Delta_{ij}^{(0)}=\sum_{k=1}^{m}B_i(x_k)B_j(y_k)\delta_k^{(0)}.$$

Define

$$\boldsymbol{\delta}_1^{(0)}=\left[\delta_1^{(0)},\delta_2^{(0)},\ldots,\delta_m^{(0)}\right]^{\mathrm{T}},$$
$$\boldsymbol{\Delta}_1{}^{(0)}=\left[\Delta_{1,1}^{(0)},\Delta_{1,2}^{(0)},\ldots,\Delta_{N,M}^{(0)}\right]^{\mathrm{T}},$$

which satisfies $\boldsymbol{\Delta}_1^{(0)}=B_1^{\mathrm{T}}\boldsymbol{\delta}_1^{(0)}$. Similarly, the difference vectors for the offset points and control coefficients can be expressed as:

$$\delta_l^{(0)}=\epsilon_1-f(x_l,y_l),\quad l=m+1,m+2,\ldots,2m,$$
$$\delta_k^{(0)}=\epsilon_2-f(x_k,y_k),\quad k=2m+1,2m+2,\ldots,3m,$$
$$\Delta_{ij}^{(0)}=\sum_{k=m+1}^{3m}B_i(x_k)B_j(y_k)\delta_k^{(0)},\quad k=m+1,m+2,\ldots,3m,$$

and they satisfy $\boldsymbol{\Delta}_2^{(0)}=B_2^{\mathrm{T}}\boldsymbol{\delta}_2^{(0)}$, $\boldsymbol{\Delta}_3^{(0)}=B_3^{\mathrm{T}}\boldsymbol{\delta}_3^{(0)}$, where B_2,B_3 are the collocation matrices of the basis functions for the offset points. The new matrix of control coefficients can then be obtained by $C^{(1)}=C^{(0)}+\mu(\boldsymbol{\Delta}_1{}^{(0)}+\boldsymbol{\Delta}_2{}^{(0)}+\boldsymbol{\Delta}_3{}^{(0)})$, and the new implicit function is

$$f^{(1)}(x,y)=\sum_{i=1}^{N}\sum_{j=1}^{M}C_{ij}^{(1)}B_i(x)B_j(y).$$

Likewise, when we obtain the α-th result, $C^{(\alpha)}$, let

$$\boldsymbol{\Delta}_1^{(\alpha)}=B_1^{\mathrm{T}}\boldsymbol{\delta}_1^{(\alpha)},$$
$$\boldsymbol{\Delta}_2^{(\alpha)}=B_2^{\mathrm{T}}\boldsymbol{\delta}_2^{(\alpha)},$$
$$\boldsymbol{\Delta}_3^{(\alpha)}=B_3^{\mathrm{T}}\boldsymbol{\delta}_3^{(\alpha)},$$
$$C^{(\alpha+1)}=C^{(\alpha)}+\mu(\boldsymbol{\Delta}_1{}^{(\alpha)}+\boldsymbol{\Delta}_2{}^{(\alpha)}+\boldsymbol{\Delta}_3{}^{(\alpha)}),$$

then the implicit function after the $(\alpha+1)$-th iteration can be expressed as:

$$f^{(\alpha+1)}(x,y)=\sum_{i=1}^{N}\sum_{j=1}^{M}C_{ij}^{(\alpha+1)}B_i(x)B_j(y).$$

Let

$$b=[\underbrace{0,0,\cdots,0}_{m},\underbrace{\epsilon_1,\epsilon_1,\cdots,\epsilon_1}_{m},\underbrace{\epsilon_2,\epsilon_2,\cdots,\epsilon_2}_{m}]^{\mathrm{T}}, \tag{9}$$

and

$$D=[B_1{}^{\mathrm{T}},B_2{}^{\mathrm{T}},B_3{}^{\mathrm{T}}]^{\mathrm{T}}, \tag{10}$$

then the I-PIA for Implicit B-spline curve reconstruction can be expressed in matrix form as

$$\begin{aligned}C^{(\alpha+1)}&=C^{(\alpha)}+\mu D^{\mathrm{T}}(B-DC)\\&=(I-\mu D^{\mathrm{T}}D)C^{(\alpha)}+\mu D^{\mathrm{T}}b.\end{aligned} \tag{11}$$

Remarkably, to ensure the convergence of (11), the weight factor μ should satisfy the following condition:

$$0<\mu<\frac{2}{\lambda_{max}}, \tag{12}$$

according to [14], where the λ_{max} is the maximum eigenvalue of $D^{\mathrm{T}}D$. In this paper, we set

$$\mu=\frac{2}{\|D^{\mathrm{T}}D\|_{\infty}}. \tag{13}$$

III. IMPLICIT CURVE RECONSTRUCTION WITH UNIFORM RATIONAL SPLINE

A. RECONSTRUCTION MODEL

In the previous section, we introduced a model and iterative process for implicit curve reconstruction with B-spline. To improve the fitting accuracy and fit more general curves, we chose to use uniform rational basis spline function instead of an implicit B-spline basis function for the reconstruction.

The nonzero implicit function $g(x,y)$ which we need is defined as follows:

$$g(x,y)=\sum_{i=1}^{N}\sum_{j=1}^{M}C_{ij}\frac{w_{ij}B_i(x)B_j(y)}{\sum_{i=1}^{N}\sum_{j=1}^{M}w_{ij}B_i(x)B_j(y)}, \tag{14}$$

where w_{ij} are non-negative weights. Thus, the resulting implicit curve can be expressed as:

$$z_g = \{(x, y) \in \Omega \subseteq \mathbb{R}^2 : g(x, y) = 0\}. \tag{15}$$

Similarly, the internal and external offset points were added to the data set. Then our problem of implicit curve reconstruction with a uniform rational spline is to find a nonzero function $g(x, y)$ to minimize the square error function:

$$\begin{aligned} E(C, w) = &\sum_{i=1}^{m} \|g(P_i)\|_2^2 \\ &+ \sum_{l=m+1}^{2m} \|g(P_l) - \epsilon_1\|_2^2 \\ &+ \sum_{k=2m+1}^{3m} \|g(P_k) - \epsilon_2\|_2^2. \end{aligned} \tag{16}$$

Then the problem could be basically equivalent to solving the optimization function:

$$\arg\min_{C,w} E(C, w), \tag{17}$$

where $w = [w_{11}, w_{12}, \ldots, w_{1M}, \ldots, w_{NM}]^{\mathrm{T}}$. In contrast to the B-spline, the iteration process for reconstruction with a uniform rational spline can be divided into iterations of weights and control coefficients.

1) ITERATION OF WEIGHTS

By introducing weights into the implicit function, the curve has a higher degree of freedom, which can improve the shape of the resulting curve and allow it to better approximate the positions of data points. Therefore, we consider the iteration of the weights.

Let

$$\begin{aligned} E(C, w) &= \sum_{k=1}^{3m} \|g(x_k, y_k) - \epsilon\|_2^2, \\ \epsilon &= \begin{cases} 0, & k = 1, 2, \ldots, m \\ \epsilon_1, & k = m+1, m+2, \ldots, 2m \\ \epsilon_2, & k = 2m+1, 2m+2, \ldots, 3m, \end{cases} \end{aligned} \tag{18}$$

the partial derivative of the objective function with respect to weights is calculated as:

$$\frac{\partial E(C, w)}{\partial w_{lm}} = 2 \times \sum_{k=1}^{3m} \langle (g(x_k, y_k) - \epsilon), \frac{\partial g(x_k, y_k)}{\partial w_{lm}} \rangle.$$

Finally, the gradient of E with respect to weigths is obtained by

$$\nabla_w E(C, w) = \left[\frac{\partial E}{\partial w_{11}}, \ldots, \frac{\partial E}{\partial w_{1M}}, \ldots, \frac{\partial E}{\partial w_{NM}} \right]^{\mathrm{T}}, \tag{19}$$

Thus the iteration of weights is expressed as

$$w^{(\alpha+1)} = w^{(\alpha)} - \tau \cdot \nabla_w E, \tag{20}$$

where τ is appropriate step size.

2) ITERATION OF CONTROL COEFFICIENTS

Similarly, we define the initial implicit function,i.e.,

$$g^{(0)}(x, y) = \sum_{i=1}^{N} \sum_{j=1}^{M} C_{ij} \frac{w_{ij} B_i(x) B_j(y)}{\sum_{i=1}^{N} \sum_{j=1}^{M} w_{ij} B_i(x) B_j(y)}. \tag{21}$$

Let $\delta_i^{(0)}$ be the difference vectors for the data points,i.e.,

$$\begin{aligned} \delta_i^{(0)} &= 0 - g(x_i, y_i), \quad i = 1, 2, \ldots, m, \\ \delta_l^{(0)} &= \epsilon_1 - g(x_l, y_l), \quad l = m+1, m+2, \ldots, 2m, \\ \delta_k^{(0)} &= \epsilon_2 - g(x_k, y_k), \quad k = 2m+1, 2m+2, \ldots, 3m. \end{aligned}$$

Maintaining the weight w^1 unchanged after the iteration of the weights, the differential vectors of the control coefficients are calculated as

$$\Delta_{ij}^{(0)} = \sum_{k=1}^{3m} \frac{w_{ij} B_i(x_k) B_j(y_k)}{\sum_{i=1}^{N} \sum_{j=1}^{M} w_{ij}^{(1)} B_i(x_k) B_j(y_k)} \delta_k^{(0)}.$$

Let

$$\begin{aligned} \boldsymbol{\Delta}^{(0)} &= \left[\Delta_{11}^{(0)}, \ldots, \Delta_{1M}^{(0)}, \ldots, \Delta_{NM}^{(0)} \right]^{\mathrm{T}} \\ &= R_1^{\mathrm{T}} \boldsymbol{\delta}_1^{(0)} + R_2^{\mathrm{T}} \boldsymbol{\delta}_2^{(0)} + R_3^{\mathrm{T}} \boldsymbol{\delta}_3^{(0)}, \end{aligned}$$

where R_1, R_2, R_3 are the collocation matrices of the basis functions for the data points and offset points, respectively.

Likewise, when we obtain the α-th result, $w^{(\alpha+1)}$, $C^{(\alpha)}$, let

$$\begin{aligned} w^{(\alpha+1)} &= w^{(\alpha)} - \tau \cdot \nabla_w E, \\ \boldsymbol{\Delta}^{(\alpha)} &= R_1^{\mathrm{T}} \boldsymbol{\delta}_1^{(\alpha)} + R_2^{\mathrm{T}} \boldsymbol{\delta}_2^{(\alpha)} + R_3^{\mathrm{T}} \boldsymbol{\delta}_3^{(\alpha)}, \\ C^{(\alpha+1)} &= C^{(\alpha)} + \mu \boldsymbol{\Delta}^{(\alpha)}, \end{aligned}$$

then the implicit function after the $(\alpha+1)$-th iteration can be expressed as:

$$\begin{aligned} &g^{(\alpha+1)}(x, y) \\ &= \sum_{i=1}^{N} \sum_{j=1}^{M} C_{ij}^{(\alpha+1)} \frac{w_{ij}^{(\alpha+1)} B_i(x) B_j(y)}{\sum_{i=1}^{N} \sum_{j=1}^{M} w_{ij}^{(\alpha+1)} B_i(x) B_j(y)}. \end{aligned} \tag{22}$$

Let

$$D = [R_1{}^{\mathrm{T}}, R_2{}^{\mathrm{T}}, R_3{}^{\mathrm{T}}]^{\mathrm{T}}, \tag{23}$$

then the curve reconstruction with uniform rational spline can be expressed in matrix form as

$$\begin{aligned} C^{(\alpha+1)} &= C^{(\alpha)} + \mu D^{\mathrm{T}}(b - DC) \\ &= (I - \mu D^{\mathrm{T}} D) C^{(\alpha)} + \mu D^{\mathrm{T}} b. \end{aligned} \tag{24}$$

To ensure the convergence of (24), μ should satisfy $0 < \mu < \frac{2}{\lambda_{max}}$, where λ_{max} is the maximum eigenvalue of $D^{\mathrm{T}}D$. Similarly, we set

$$\mu = \frac{2}{\|D^{\mathrm{T}} D\|_\infty}. \tag{25}$$

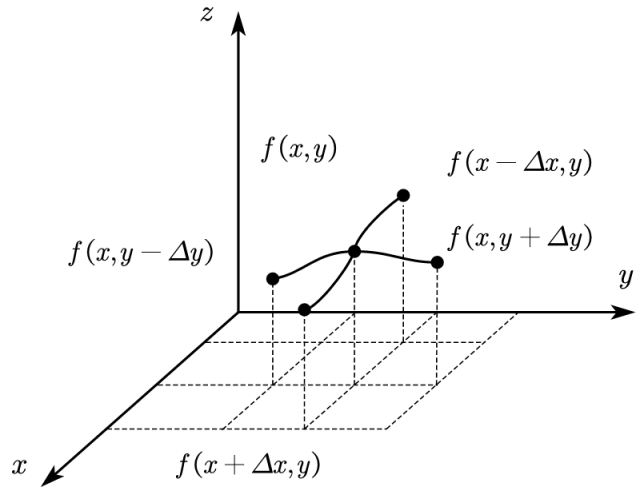

FIGURE 1. Variations around (x, y) on recondtructed surface.

IV. REGULARIZATION TERM TO DECREASE THE SUPPLEMENTARY ZERO-LEVEL SETS

A. THE CONSTRUCTION OF REGULARIZATION TERM

In curve reconstruction problems, the presence of supplementary zero-level sets often arises because of the intersection between the reconstructed curve and zero-level set. This is an unresolved issue in curve reconstruction. Liu et al. [17] provided a solution for this problem. In this paper, we propose a method based on minimizing the oscillation function of the reconstructed surface to modify the properties of the constructed surface and make it as smooth as possible, thereby reducing the occurrence of supplementary intersection points between the reconstructed surface and zero-level set.

Regarding the constructed implicit surface, the constraint conditions can only be applied to the given data points and their corresponding offset points. However, there is a lack of constraints in the other regions inside and outside the curve. Therefore, supplementary zero-level sets are likely to occur in these areas.

Therefore, we define an oscillation function $S_{\Omega_1}(f(x,y))$ to show the oscillation around $(x, y) \in \Omega_1$ on the reconstructed surface as follows:

$$\begin{aligned} S_{\Omega_1}(f(x,y)) = [&(f(x+\Delta x,y)-f(x,y))^2 \\ &+(f(x-\Delta x,y)-f(x,y))^2 \\ &+(f(x,y+\Delta y)-f(x,y))^2 \\ &+(f(x,y-\Delta y)-f(x,y))^2]/16. \end{aligned} \tag{26}$$

In Fig. 1, $S_{\Omega_1}(f(x,y))$ reflects the smoothness around (x, y) on the surface to a certain extent. The greater the $S_{\Omega_1}(f(x,y))$, the greater the oscillation around (x, y) on the surface, and the more likely it is to intersect with the zero-level set to appear as supplementary level sets.

Define the oscillation function on Ω as:

$$S_\Omega(f) = \frac{1}{16}\int_\Omega (f_x^2 + f_{-x}^2 + f_y^2 + f_{-y}^2)dxdy. \tag{27}$$

For cubic B-spline curve function, we have:

$$\begin{aligned} |f'| &= n|\sum_{i=0}^{N-1} \frac{c_{i+1}-c_i}{t_{i+n+1}-t_{i+1}} B_{i+1}(t)| \\ &\le \frac{n}{min_i\{t_{i+n+1}-t_{i+1}\}} \sum_{i=0}^{N-1} |C_{i+1}-C_i| \\ &= c_1 \sum_{i=0}^{N-1} |C_{i+1}-C_i|. \end{aligned} \tag{28}$$

So that we can make an estimation as follows:

$$\begin{aligned} &f_x^2 + f_{-x}^2 + f_y^2 + f_{-y}^2 \\ &\le c_1[(\sum_{ij}|C_{i+1,j}-C_{ij}|)^2 + (\sum_{ij}|C_{i-1,j}-C_{ij}|)^2 \\ &\quad + (\sum_{ij}|C_{i,j+1}-C_{ij}|)^2 + (\sum_{ij}|C_{i,j-1}-C_{ij}|)^2] \\ &\le c_2[\sum_{ij}|C_{i+1,j}-C_{ij}|^2 + \sum_{ij}|C_{i-1,j}-C_{ij}|^2 \\ &\quad + \sum_{ij}|C_{i,j+1}-C_{ij}|^2 + \sum_{ij}|C_{i,j-1}-C_{ij}|^2] \\ &= c_2 \sum_{ij}(|C_{i+1,j}-C_{ij}|^2 + |C_{i+1,j}-C_{ij}|^2 \\ &\quad + |C_{i+1,j}-C_{ij}|^2 + |C_{i+1,j}-C_{ij}|^2) \\ &\triangleq c_2 \sum_{ij} ||\mathcal{R}C_{ij}||^2, \end{aligned} \tag{29}$$

where c_1, c_2 are nonzero constants, c_1 can be derived from (28), and c_2 can be obtained by Cauchy-Schwarz inequality. Let $\mathcal{R}$ be the difference operator of the control coefficients:

$$\begin{aligned} &\frac{1}{16}\int_\Omega (f_x^2 + f_{-x}^2 + f_y^2 + f_{-y}^2)dxdy \\ &\le c_2 \sum_{ij} ||\mathcal{R}C_{ij}||^2 \cdot \int_\Omega dxdy \\ &= c_2|\Omega| \sum_{ij} ||\mathcal{R}C_{ij}||^2 \\ &\triangleq \tilde{c} \sum_{ij} ||\mathcal{R}C_{ij}||^2. \end{aligned} \tag{30}$$

In particular, when $\mathcal{R}C_{ij}$ is invalid, meaning that some of its elements exceed the index range, we set the corresponding control coefficient difference to zero, for example,

$$\mathcal{R}C_{11} = (C_{21}-C_{11}, 0, C_{12}-C_{11}, 0)^{\mathrm{T}}.$$

Thus, we have an estimation of the oscillation function on Ω as in (30). When the reconstructed surface oscillation tended to zero, $f_x^2 + f_{-x}^2 + f_y^2 + f_{-y}^2$ also tended to zero. The oscillation function can be effectively approximated using a matrix composed of the differences in the control coefficients. Then, the problem is to move the control coefficients C_{ij} to

minimize the function:

$$R(C) = \sum_{ij} \|\mathcal{R}C_{ij}\|_2^2. \tag{31}$$

B. UPDATE ITERATION MODEL

After incorporating the regularization term, the objective function is updated as follows:

$$\arg\min_{C,w} E(C, w) + \lambda R(C), \tag{32}$$

where λ denotes the appropriate step size. Similarly, the iteration of weights remains the same as in (20), and the iteration of the control coefficients updates correspondingly as follows:

$$C^{(\alpha+1)} = C^{(\alpha)} + \mu D^{\mathbf{T}}(b - DC) - \lambda \nabla_C R(C), \tag{33}$$

where the gradient of the regularization term with respect to the control coefficients is obtained as follows:

$$\nabla_C R(C) = \left[\frac{\partial R(C)}{\partial C_{11}}, \ldots, \frac{\partial R(C)}{\partial C_{1M}}, \ldots, \frac{\partial R(C)}{\partial C_{NM}}\right]. \tag{34}$$

V. EXPERIMENT

During the iterative process, we set following evaluation metrics:

1) E shows the energy of iteration:

$$E = \|R_1 C\|_2^2 + \|R_2 C\|_2^2 + \|R_3 C\|_2^2 + \lambda R(C). \tag{35}$$

2) E_{ave} shows average error:

$$E_{ave} = \frac{1}{m}\|R_1 C\|_2^2. \tag{36}$$

3) E_{max} shows relative maximum error:

$$E_{max} = max(|R_1 C|). \tag{37}$$

Let $\Delta E = |E_{new} - E_{old}|$ be the iterative error between adjacent iterations. The iteration is stopped when ΔE satisfies

$$\Delta E < e_{tolerance}, \tag{38}$$

or the maximum number of iterations is reached.

A. ALGORITHM OF RECONSTRUCTION METHOD WITH REGULARIZATION TERM

Based on the above indicators, the pseudo-code of the optimization algorithm is given as follows:

Algorithm 1 Implicit Uniform Rational Spline Reconstruction Method With Regularization Term

Input: $\{P_i\}_{i=1}^m$: Data points;
$\{d_i\}_{i=1}^2$, $\{\epsilon_i\}_{i=1}^2$: Internal and external offsets and corresponding offsets of function;
Grid size;
K_{max}: Maximum iterations;
$e_{tolerance}$: Error tolerance for convergence.
Output: Evaluation metrics(E, E_{ave}, E_{max}, $R(C)$);
C: Control coefficient matrix;
w: Weight matrix.
Set all the initial control coefficients $C_{ij}^{(0)}$ to 0 and all the weights $w_{ij}^{(0)}$ to 1.0;
Construct uniform knot vector according to grid size;
Construct collocation matrixs of the basis functions for data points and offset points R_1, R_2, R_3, and constitute **D** by (23);
Compute the initial energy of iteration : $E^{(0)}$;
for $k = 0; k < K_{max}, ++k$ **do**
  Compute $R(C)$ by (31) and $\nabla_C R(C)$ by (34);
  Update $w^{(k+1)}$ by solving (20);
  Update $C^{(k+1)}$ by solving (33);
  Reconstruct R_1, R_2, R_3, and constitute **D** by (23);
  Compute the energy $E^{(k+1)}$ by (35)
  if $|E^{(k+1)} - E^{(k)}| < e_{tolerance}$ **then**
    Compute E_{ave}, E_{max} by (36), (37);
    return $R(C)$, E, E_{ave}, E_{max}.
  end if
end for

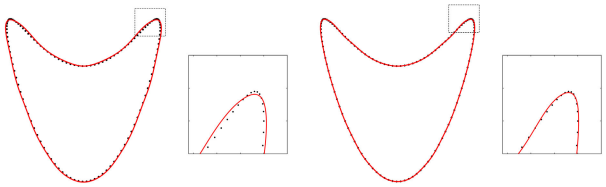

(a) Reconstruction with B-spline (b) Reconstruction with uniform rational spline

FIGURE 2. The reconstruction results of Example 1.

B. RESULTS

Example 1: 120 data points sampled from the curve which is defined as follows

$$\begin{cases} x = 4cos(t), \\ y = sin(t)(3 - 5sin(t)), \end{cases} \quad t \in [0, 2\pi].$$

The grid size is $9 * 9$, the internal and external offsets are 0.1 and the corresponding offsets of the function are -0.01 and 0.01, respectively. We set $\tau =$ 1e-2. Both under 200 iterations, Fig. 2(a) and Fig. 2(b) show the comparison of the reconstruction result with B-spline and that with uniform rational spline.

Example 2: 193 data points are sampled from the figure.

The internal and external offsets are 0.1 and the corresponding offsets of the function are -0.01 and 0.01, respectively. Two different methods were used to reconstruct the curves of grid sizes 10*10 and 15*15 respectively. Under 200 iterations, we set $\tau =$ 1e-2.

Fig. 3 and Fig. 4 show the results of our algorithm without regularization term. When the grid scale increased, the results of the curve reconstruction noticeably improved. Under the same number of iterations, the implicit reconstruction method with a uniform rational spline had a smaller average error. Furthermore, for the same grid size (Fig. 3(a) and Fig. 3(b),

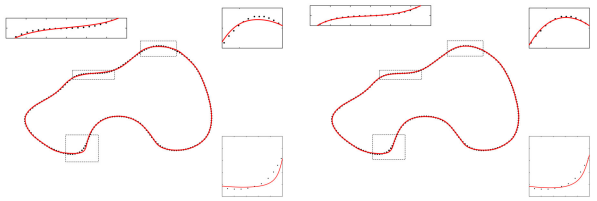

(a) Reconstruction with B-spline (b) Reconstruction with uniform rational spline

FIGURE 3. The reconstruction results of Example 2(10*10).

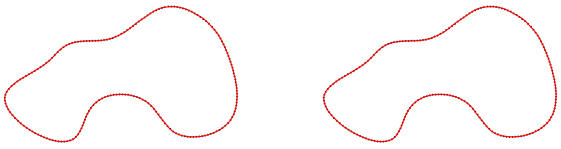

(a) Reconstruction with B-spline (b) Reconstruction with uniform rational spline

FIGURE 4. The reconstruction results of Example 2(15*15).

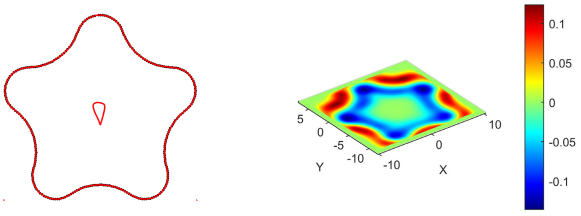

FIGURE 5. The reconstruction results without regularization term of Example 3.

details in Table 1), the method with uniform rational spline outperforms better in fitting accuarcy and shaping details.

When a higher accuracy is required for curve reconstruction, it often leads to the presence of supplementary zero-level sets owing to insufficient constraints. To address this issue, we introduce a regularization term to reduce the presence of extra zero-level sets. In the following examples, we set

$$e_{tolerance} = 1e - 7.$$

Meanwhile, to demonstrate the improvements resulting from altering the spline basis functions and incorporating regularization terms, we set

$$\eta = |\frac{E - E'}{E}| \times 100\%,$$

where E' represents the evaluation metric with either uniform rational splines or a regularization term, whereas E does not include them. The larger η is, the better the optimization effect of our improvement is, and vice versa.

Example 3: 289 data points are sampled from the figure.

The grid size is $13*13$, internal and external offsets are 0.1, and the corresponding offsets of the function are -0.01 and 0.01. We set $\lambda = 0.0142$ and $\tau = 1e - 3$. Under the same iteration accuracy, the iteration results with and without the regularization terms are as follows:

Example 4: 639 data points are sampled from the figure.

The grid size is $15*15$, internal and external offsets are 0.1, and the corresponding offsets of the function are -0.01 and 0.01. We set $\lambda = 0.0216$ and $\tau = 1e - 3$. Under the same

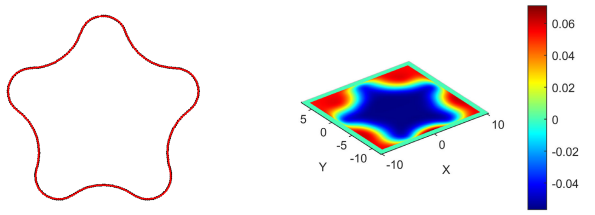

FIGURE 6. The reconstruction results with regularization term of Example 3.

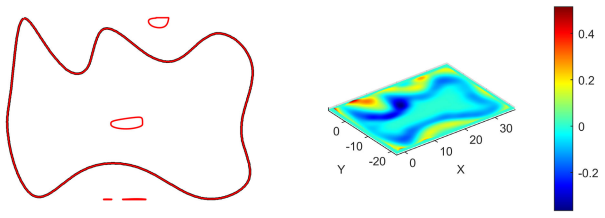

FIGURE 7. The reconstruction results without regularization term of Example 4.

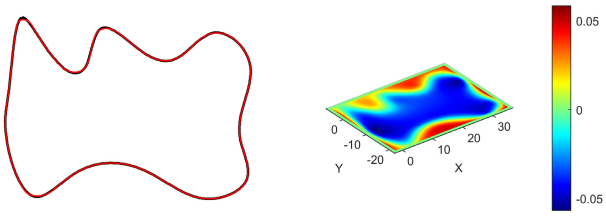

FIGURE 8. The reconstruction results with regularization term of Example 4.

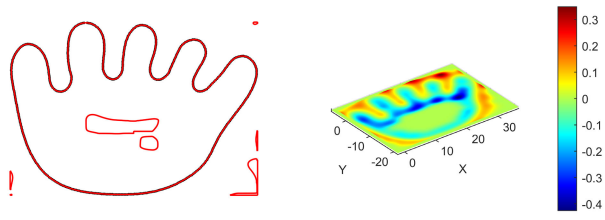

FIGURE 9. The reconstruction results without regularization term of Example 5.

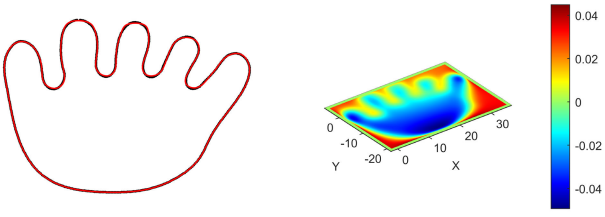

FIGURE 10. The reconstruction results with regularization term of Example 5.

iteration accuracy, the iteration results with and without the regularization terms are as follows:

Example 5: 595 data points are sampled form the figure.

The grid size is $17*17$, internal and external offsets are 0.1, and the corresponding offsets of the function are -0.01 and 0.01. We set $\lambda = 0.0242$ and $\tau = 1e - 3$. Under the same iteration accuracy, the iteration results with and without the regularization terms are as follows:

Example 6: 400 data points are sampled from the figure.

TABLE 1. Reconstruction result of Example 1 and Example 2.

	Grid size	Spline	E	E_{max}	E_{ave}	Iterations
Example 1	9*9	B-spline	9.4303e-04	2.1919e-03	1.2682e-06	200
	9*9	uniform rational spline	1.63e-03	2.3667e-03	8.4608e-07	200
Example 2	10*10	B-spline	1.6885e-03	2.2504e-03	5.2849e-07	200
	10*10	uniform rational spline	1.0754e-03	2.1599e-03	5.0631e-07	200
	15*15	B-spline	6.3317e-03	2.5553e-03	4.9329e-07	200
	15*15	uniform rational spline	6.3264e-03	2.5564e-03	4.9355e-07	200

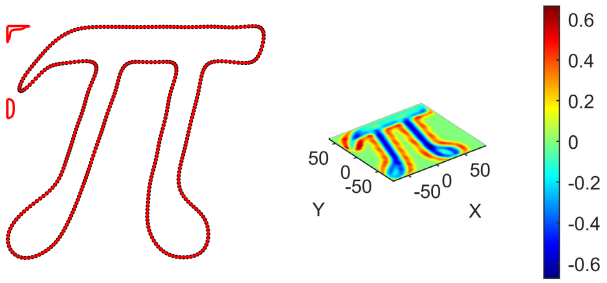

FIGURE 11. The reconstruction results without regularization term of Example 6.

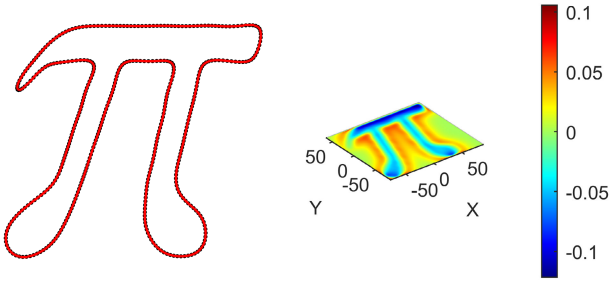

FIGURE 12. The reconstruction results with regularization term of Example 6.

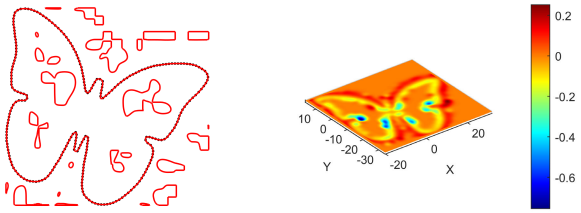

FIGURE 13. The reconstruction results without regularization term of Example 7.

The grid size is $25 * 25$, the internal and external offsets are 0.1, and the corresponding offsets of the function are -0.01 and 0.01. We set $\lambda = 0.00425$ and $\tau = 1e-3$. Under the same iteration accuracy, the iteration results with and without the regularization terms are as follows:

Example 7: 262 data points are sampled from the figure.

The grid size is $28 * 28$, the internal and external offsets are 0.1, and the corresponding offsets of the function are -0.01 and 0.01. We set $\lambda = 0.00215$ and $\tau = 1e-3$. Under the same iteration accuracy, the iteration results with and without regularization terms are as follows:

To visualize the changes in the reconstructed surface during the iterative process, we present four iteration states of the method with the regularization term in Example 6 as follows:

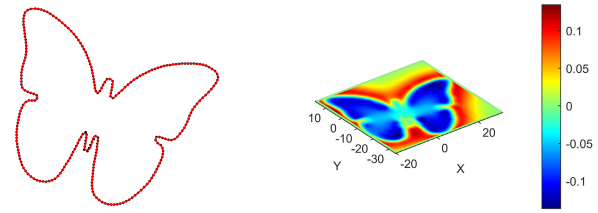

FIGURE 14. The reconstruction results with regularization term of Example 7.

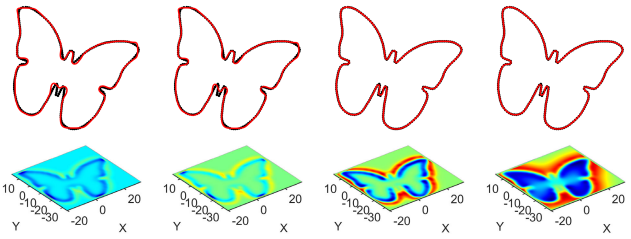

FIGURE 15. Four states of reconstrction with regularization term.

The above experimental results demonstrate the reconstructed curves and heatmaps of the surfaces on a two-dimensional plane. From the results and the data in Table 2, it can be seen that adding a regularization term could avoid unnecessary intersection between the surface and the zero-level set during the iteration process, making the generated surface smoother and achieving the fitting target. In addition, the value of the regularization term is effectively reduced. Fig. 15 shows the change in the reconstructed surface during the iteration process after adding the regularization term. Owing to the effect of the regularization term on the surface, no supplementary zero-level set was created between the surface and the zero set during the reconstruction process.

Furthermore, to evaluate the efficacy of our regularization term, we conducted a sensitivity analysis of the coefficient λ of the regularization term.

Example 8: In Example 7, we apply our method to curve reconstruction. By keeping the other parameters unchanged, λ was varied from 0.001 to 0.006. Table 3 and Fig. 16 present the results.

In fact, more point cloud data is not so regular, so for data points with noise, we are more concerned about whether the algorithm can run normally. Let us consider the curve reconstruction problem in which the initial data points are affected by noise.

Example 9: For example 1, we use algorithms to reconstruct the curve for 400 noisy data points. Under the same

TABLE 2. Reconstruction result of Example 3 to 6.

	With or without regularization term	E_{max}	E_{ave}	η for E_{ave}	$R(\mathbf{C})$	CPU time
Example 3	without	2.8381e-03	1.0685e-06		0.42102	0.62724
	with	2.1732e-03	5.4473e-07	49.02%	0.021446	0.45154
Example 4	without	2.926e-03	1.0636e-06		2.0729	40.443
	with	2.3465e-03	3.4776e-07	67.30%	0.027086	1.1551
Example 5	without	3.0942e-03	1.1554e-06		2.6316	111.625
	with	2.4792-03	3.377e-07	70.77%	0.021446	1.4585
Example 6	without	2.2292e-03	2.0638e-07		22.4046	41.1254
	with	1.0078e-03	4.4867e-08	78.26%	0.17126	2.9149
Example 7	without	4.3134e-03	2.1195e-06		2.4451	7.0922
	with	3.7598e-03	1.2299e-06	41.97%	0.40428	3.8809

TABLE 3. Value of evaluation metrics while λ varies.

	λ	E_{max}	E_{ave}	CPU time
Example 8	0.001	0.0011751	8.3627e-08	5.9182
	0.002	0.0010719	5.9692e-08	3.8041
	0.003	0.0010484	5.0708e-08	2.9848
	0.004	0.0010163	4.5794e-08	2.6653
	0.005	0.00098191	4.2509e-08	2.213
	0.006	0.00096713	4.0041e-08	1.9477

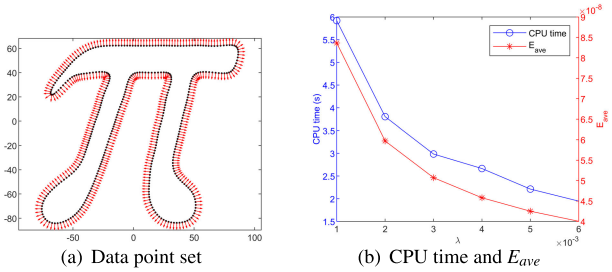

(a) Data point set (b) CPU time and E_{ave}

FIGURE 16. Sensitivity annalysis while λ varies.

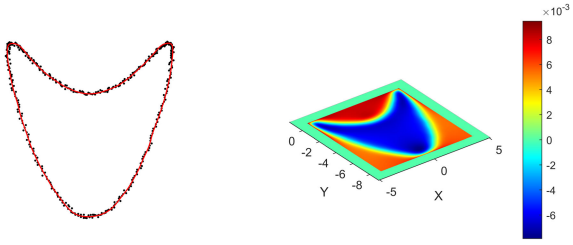

FIGURE 17. The reconstruction results with regularization term of Example 9.

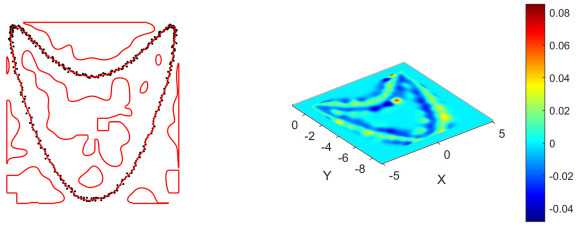

FIGURE 18. The reconstruction results without regularization term of Example 9.

parameters as those in Example 1, the grid size is $20 * 20$ and $\lambda = 0.512$. The details are as follows:

Example 10: For the original curve without noise:

$$\begin{cases} x = 4cos(t), \\ y = 5sin(t), \end{cases} \qquad t \in [0, 2\pi].$$

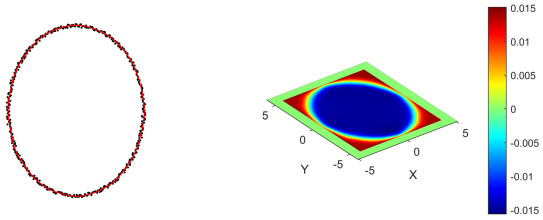

FIGURE 19. The reconstruction results with regularization term of Example 10.

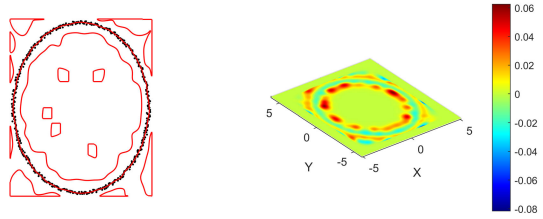

FIGURE 20. The reconstruction results without regularization term of Example 10.

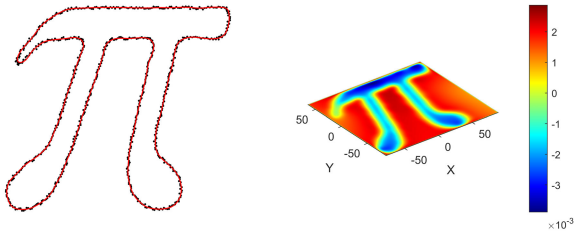

FIGURE 21. The reconstruction results with regularization term of Example 9

We use algorithms to reconstruct the curve for 500 noisy data points. The grid size is $20 * 20$, the internal and external offsets are 0.1 and the corresponding offsets of the function are -0.01 and 0.01, respectively. We set $\tau =$ 1e-2 and $\lambda = 0.314$. The details are as follows:

Example 11: For example 6, we use algorithms to reconstruct the curve for 800 data points with noise. Under the same parameters as those in Example 6, the grid size is $25 * 25$ and $\lambda = 0.134$. The details are as follows:

In Examples 9 to 11, the results indicate that the algorithm demonstrates strong robustness when applied to datasets with noise. Additionally, in Table 4, the I-PIA method takes more time to process noisy data, which is indicative of overfitting. By contrast, the algorithm with the regularization term is more efficient and consumes less time. Furthermore, the algorithm can ensure smoothness of the reconstructed curve.

TABLE 4. Value of the evaluation metrics while λ varies.

	With or without regularization term	$R(C)$	E_{ave}	CPU time (s)
Example 9	with	0.00079967	1.3119e-06	0.32538
	without	0.21634	1.3901e-05	5.2778
Example 10	with	0.0024841	3.8785e-06	0.81149
	without	0.25325	1.5749e-05	9.2066
Example 11	with	0.17914	1.9002e-06	30.5346
	without	1.93E-04	1.3179e-07	1.4799

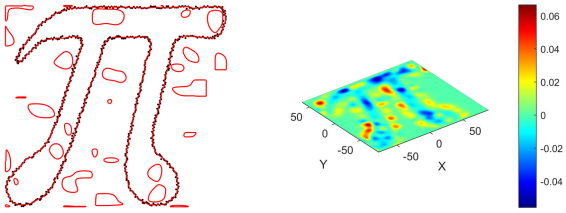

FIGURE 22. The reconstruction results without regularization term of Example 9.

VI. DISCUSSION AND CONCLUSION

This paper proposes a method for implicit curve reconstruction based on uniform rational splines and provides the corresponding weight iteration and control coefficient iteration formats. With increased degrees of freedom, this method could achieve higher accuracy in reconstructing the target curve, compared to the traditional implicit B-spline reconstruction(I-PIA). Furthermore, the algorithm demonstrates superior robustness when applied to noisy datasets. The reconstruction process is more concise, whereas the I-PIA algorithm would overfit. Moreover, the introduction of a regularization term enhances the smoothness of the reconstructed surface. By incorporating the regularization term, the occurrence of supplementary zero-level sets in the results is minimized compared to the iteration process without a regularization term. Consequently, the reconstructed curve demonstrates a higher accuracy while maintaining the same level of iteration precision.

REFERENCES

[1] T. Weihua, "A surface reconstruction algorithm based on implicit T-spline surfaces," *J. Comput. Aided Des. Comput. Graph.*, vol. 18, no. 3, p. 358, 2006.
[2] S. Cuomo, A. Galletti, G. Giunta, and L. Marcellino, "Reconstruction of implicit curves and surfaces via RBF interpolation," *Appl. Numer. Math.*, vol. 116, pp. 157–171, Jun. 2017.
[3] H. Wang, T. Liu, S. Liu, W. Wei, X. Liu, P. Liu, Y. Bai, and Y. Chen, "Implicit progressive-iterative algorithm of curves and surfaces with compactly supported radial basis functions," *J. Comput.-Aided Des. Comput. Graph.*, vol. 33, no. 11, pp. 1755–1764, Nov. 2021.
[4] L. Lan, Y. Ji, M.-Y. Wang, and C.-G. Zhu, "Full-LSPIA: A least-squares progressive-iterative approximation method with optimization of weights and knots for NURBS curves and surfaces," *Comput.-Aided Des.*, vol. 169, Apr. 2024, Art. no. 103673.
[5] G. Costa, M. Montemurro, and J. Pailhès, "A general hybrid optimization strategy for curve fitting in the non-uniform rational basis spline framework," *J. Optim. Theory Appl.*, vol. 176, no. 1, pp. 225–251, Jan. 2018.
[6] G. Bertolino, M. Montemurro, N. Perry, and F. Pourroy, "An efficient hybrid optimization strategy for surface reconstruction," in *Proc. Comput. Graph. Forum*, vol. 40, 2021, pp. 215–241.
[7] X. Zhao, C. Zhang, B. Yang, and P. Li, "Adaptive knot placement using a GMM-based continuous optimization algorithm in B-spline curve approximation," *Comput.-Aided Des.*, vol. 43, no. 6, pp. 598–604, Jun. 2011.
[8] A. Gálvez and A. Iglesias, "Particle swarm optimization for non-uniform rational B-spline surface reconstruction from clouds of 3D data points," *Inf. Sci.*, vol. 192, pp. 174–192, Jun. 2012.
[9] D. Qi, Z. Tian, Y. Zhang, and J. B. Zheng, "The method of numeric Polish in curve fitting," *Acta Math. Sinica*, vol. 18, no. 3, pp. 173–184, 1975.
[10] C. de Boor, "How does Agee's smoothing method work?" in *Proc. Army Numer. Anal. Comput. Conf.*, 1979, pp. 299–302.
[11] H. Lin, G. Wang, and C. Dong, "Constructing iterative non-uniform B-spline curve and surface to fit data points," *Sci. China Ser., Inf. Sci.*, vol. 47, pp. 315–331, May 2004.
[12] H.-W. Lin, H.-J. Bao, and G.-J. Wang, "Totally positive bases and progressive iteration approximation," *Comput. Math. Appl.*, vol. 50, nos. 3–4, pp. 575–586, Aug. 2005.
[13] H. Lin and Z. Zhang, "An extended iterative format for the progressive-iteration approximation," *Comput. Graph.*, vol. 35, no. 5, pp. 967–975, Oct. 2011.
[14] C. Deng and H. Lin, "Progressive and iterative approximation for least squares B-spline curve and surface fitting," *Comput.-Aided Des.*, vol. 47, pp. 32–44, Feb. 2014.
[15] M. Kazhdan, M. Bolitho, and H. Hoppe, "Poisson surface reconstruction," in *Proc. 4th Eurographics Symp. Geometry Process.*, vol. 7, 2006, pp. 1–10.
[16] M. Rouhani and A. D. Sappa, "Implicit B-spline fitting using the 3L algorithm," in *Proc. 18th IEEE Int. Conf. Image Process.*, Sep. 2011, pp. 893–896.
[17] Y. Liu, Y. Song, Z. Yang, and J. Deng, "Implicit surface reconstruction with total variation regularization," *Comput. Aided Geometric Des.*, vol. 52, pp. 135–153, Mar. 2017.
[18] Y. F. Hamza, H. Lin, and Z. Li, "Implicit progressive-iterative approximation for curve and surface reconstruction," *Comput. Aided Geometric Des.*, vol. 77, Feb. 2020, Art. no. 101817.
[19] H. Wang, "Implicit randomized progressive-iterative approximation for curve and surface reconstruction," *Comput.-Aided Des.*, vol. 152, Nov. 2022, Art. no. 103376.
[20] J. Song, H. Pan, Y. Zhang, W. Lu, J. Ding, W. Wei, W. Liu, Z. Pan, and J. Duan, "Three-dimensional surface reconstruction from point clouds using Euler's elastica regularization," *Appl. Sci.*, vol. 13, no. 23, p. 12695, Nov. 2023.
[21] J. Kangsong, S. Huahao, and L. Yan, "Implicit curve reconstruction with normal constraint using progressive and iterative approximation," *J. Comput.-Aided Des. Comput. Graph.*, vol. 35, no. 5, pp. 719–725, 2023.
[22] D. Zhong, J. Zhang, and L. Wang, "Fast implicit surface reconstruction for the radial basis functions interpolant," *Appl. Sci.*, vol. 9, no. 24, p. 5335, Dec. 2019.
[23] K. P. Drake, E. J. Fuselier, and G. B. Wright, "Implicit surface reconstruction with a curl-free radial basis function partition of unity method," *SIAM J. Sci. Comput.*, vol. 44, no. 5, pp. 3018–3040, Oct. 2022.

SHENGHAN HUANG received the bachelor's degree in applied mathematics from the South China University of Technology. Throughout his bachelor's studies, he demonstrated profound interest and exceptional prowess in addressing complex geometric problems, particularly in optimizing design processes through computational techniques.